

A modified profust-performance-reliability algorithm and its application to dynamic systems

Zhiyao Zhao*, Quan Quan and Kai-Yuan Cai

School of Automation Science and Electrical Engineering, BeiHang University, Beijing, China

Abstract. In the field of system health monitoring, system performance degradation or fault occurrence will decrease the system reliability to some degree. However, traditional reliability analysis is of limited usefulness in evaluating the reliability of an individual product under dynamic operating and environmental conditions. In this case, research on performance reliability as well as real-time reliability has attracted extensive attentions. Considering the characteristics of fuzzy reliability theory, a performance reliability based on profust reliability theory has its advantage on tracking system's continuous degradation. On the basis of our previous work, this paper proposes a modified profust-performance-reliability (PPR) algorithm as a supplement to the profust reliability based approach to prognostics and health management. In the modified PPR algorithm, the item of transition probability among system's multi-states is replaced with the real-time distribution of system's health status, which achieves an easier implementation of PPR's calculation in practice with higher real-time capability and accuracy. Then, its application in the performance evaluation and prediction of dynamic systems are comprehensively proposed. Finally, a simulation of a quadrotor with partial loss of actuator effectiveness is presented to validate the availability and effectiveness of the proposed method.

Keywords: Profust reliability, performance reliability, system degradation, health monitoring, quadrotor

1. Introduction

System health monitoring (SHM) has been highly concerned in the system engineering field, where information extracted from SHM can be used to understand the system behavior and improve the system utilization based on optimal component replacement and maintenance strategies [1]. In the field of SHM, the system degradation is identified by comparing the system's real-time performance with its normal operational performance [2], and system degradation or fault occurrence will lead to a decrease

of the system reliability. Thus, it is reasonable to relate the system reliability with its performance.

In the performance reliability research, the system degradation is firstly modeled based on the information extracted from some system or component variables which are highly correlated with the system performance [3–5]. Then, the performance reliability is defined and calculated with the distribution of system variables at a specific time index during the operation life. Reference [6] comprehensively reviewed the existing performance reliability analysis methods, which were classified into two types in terms of system degradation modeling method: the time series analysis [3, 4] and the regression analysis [7]. Besides the two methods above, some efforts have been made in the performance reliability

*Corresponding author. Zhiyao Zhao, School of Automation Science and Electrical Engineering, BeiHang University, Beijing 100191, China. Tel.: +86 15810288441; E-mail: zzy_buaa@buaa.edu.cn.

research based on the stochastic process analysis and the filtering-based method [6–12]. In the stochastic process analysis, the system degradation path is modeled as a stochastic process, such as the Markov chain [8, 9], or the Wiener process [10, 11]. Then, the performance reliability is calculated using the Bayes' theorem. For the filtering-based method, a system model containing system performance variables is always firstly obtained. Then, Kalman filtering [4] or particle filtering [6, 12] is employed to estimate and predict the distribution of performance variables, and the performance reliability is calculated on this basis. In [6], a modified particle filtering algorithm was proposed to estimate the system fault in a non-linear model of a three-vessel water tank system. Then, the exponential smoothing method was effectively used to achieve fault prediction, and system's performance reliability was calculated according to the fault prediction results by using the Monte Carlo strategy.

By reviewing the research above, a system or product is always considered to be failed when the corresponding performance variable reaches a predetermined and fixed threshold, and the performance reliability is defined on the binary failure threshold. Actually, a system evolving from normal to failure goes through a series of degradation states. It is inappropriate to characterize the system degradation with a fixed failure threshold. According to this, reference [13] defined the performance reliability based on an adaptive failure threshold and the distribution of performance degradation data. Comparing with a fixed failure threshold, an adaptive one is relatively flexible. Nevertheless, a definition of performance reliability based on a binary failure threshold is still of limited usefulness in characterizing the system continuous degradation to some degree, especially for a complex system which can work in a degraded condition. As a part of fuzzy reliability theory [14–21], profust reliability theory extends the traditional binary state space $\{0, 1\}$ to the fuzzy state space $[0, 1]$, and models fuzzy state transitions for a component or system representing various degrees of success and failure. Therefore, a performance reliability definition based on profust reliability theory has its advantage on tracking continuous degradation for a system or product. On the basis of [14, 15], a novel profust reliability algorithm was proposed in our previous paper [22], which can be viewed as a definition of performance reliability based on profust reliability theory, namely profust-performance-reliability (PPR) here. In [22],

the implementation process of the system health evaluation and prediction was comprehensively presented by using the PPR as a health indicator, where transition probabilities among fuzzy system states acted as an essential role in the definition of PPR. For the PPR's calculation, the transition probability among system's multi-states was dynamically acquired in the PPR evaluation process based on statistical results rather than a predetermined and fixed value. This was more suitable in the real-time performance evaluation, but still inaccurate and insufficient to reflect the system degradation without abundant data samples. Furthermore, the PPR prediction process was based on the update of transition probabilities, which was somewhat complex to implement and time-consuming. This leads to an inconvenience of real-time SHM in engineering applications. Also, it should be noted that the PPR evaluation and prediction presented in [22] was a pure data-driven method, which may decrease the evaluation and prediction accuracy without taking the system model information into consideration.

For such a purpose, this paper proposes a modified PPR algorithm, where the item of transition probability among system's multi-states is replaced with the real-time distribution of system's health status. Then, the application of the proposed algorithm in the performance evaluation and prediction of dynamic systems is comprehensively proposed. For a dynamic system, the performance reliability has its ability to describe the system performance, whereas it is difficult to define and also difficult to calculate. In this paper, the performance reliability of the dynamic system is defined on the performance reliability of its system-state-variables (SSVs), where a single SSV's performance reliability is calculated by the proposed PPR algorithm. In detail, for the system performance evaluation, Extended Kalman filtering (EKF) is firstly employed to estimate the real-time distribution of SSVs with a dynamic system model, where both the mean values and error variances of SSVs are obtained. Then, the real-time health status distribution of each SSV is obtained based on the estimated SSV's distribution and its health status classification. On this basis, the performance reliability of each SSV is calculated with the modified PPR algorithm in real time, and the performance reliability of a dynamic system is evaluated by the results of each SSV's PPR. For the process of system performance prediction, an exponential smoothing method is employed to predict the distribution of SSVs, and a similar PPR calculation process is performed.

In order to validate the availability and effectiveness of the proposed method, a simulation of a quadrotor with partial loss of actuator effectiveness is presented. A quadrotor is a multirotor helicopter that is lifted and propelled by four rotors. It is classified as rotorcraft, as opposed to fixed-wing aircraft, because their lift is generated by a set of rotors (vertically oriented propellers). By changing the speed of each rotor it is possible to specifically generate a desired total thrust; to locate for the center of thrust both laterally and longitudinally; and to create a desired total torque, or turning force. Recently, more and more quadrotors are adopted in both military and civil applications such as search and rescue, border patrol, military surveillance and agricultural production. A fault or failure in any part of the quadrotor may lead to catastrophic disasters. Therefore, in order to ensure safety, it is necessary for a quadrotor to have a performance evaluation and prediction module so that it can automatically change the control strategy and mission planning after detecting a performance anomaly.

This paper makes three major contributions. First, this paper proposes a modified system performance evaluation and prediction method based on profust reliability theory, which is a supplement to the profust reliability based approach to Prognostics and Health Management (PHM) presented in [22]. Compared to our previous work [22], the modified PPR algorithm is easier to implement with a higher real-time capability and accuracy in practice. Secondly, this paper applies the modified PPR-based PHM approach to practical dynamic systems, where the comprehensive process of the system performance evaluation and prediction method is put forward. This work characterizes the performance of a dynamic system and its SSVs with a unified health indicator, namely PPR. Thirdly, the modified PPR-based system performance evaluation and prediction method takes model information of the studied objective into account, which is an improvement of a pure data-driven method presented in [22].

The remainder of this paper is organized as follows. Section 2 proposes the theory of the modified PPR algorithm. Section 3 presents the whole implementation process of the performance evaluation and prediction of dynamic systems. Section 4 uses a case of quadrotor with partial loss of actuator effectiveness to simulate the proposed algorithm presented in Section 2 and the implementation process presented in Section 3, where simulation results are given and discussed. Section 5 gives a conclusion, and indicates future development of the proposed method.

2. Theory of modified PPR algorithm

For a discrete domain $U = \{S_1, S_2, \dots, S_n\}$. In the domain U , fuzzy success states are defined as

$$S = \{S_i, \mu_S(S_i); S_i \in U\},$$

and fuzzy failure states are defined as

$$F = \{S_i, \mu_F(S_i); S_i \in U\}.$$

Without loss of generality, it is usually considered that

$$\mu_S(S_i) = 1 - \mu_F(S_i), S_i \in U.$$

where $\mu_S(S_i)$ and $\mu_F(S_i)$ are success and failure membership functions of fuzzy state, respectively. Let $U_T = \{m_{ij}, i, j = 1, \dots, n\}$, where m_{ij} represents the transition from state S_i to state S_j . In the domain U_T , a transition from a fuzzy success state to a fuzzy failure state is defined as [14]

$$T_{SF} = \{m_{ij}, \mu_{T_{SF}}(m_{ij}); S_i, S_j \in U\}.$$

Here, T_{SF} is viewed as a fuzzy event, and its corresponding membership function $\mu_{T_{SF}}(m_{ij})$ is determined as [14]

$$\mu_{T_{SF}}(m_{ij}) = \begin{cases} \beta_{F|S}(S_j) - \beta_{F|S}(S_i) & \text{if } \beta_{F|S}(S_j) > \beta_{F|S}(S_i) \\ 0 & \text{otherwise} \end{cases},$$

where

$$\beta_{F|S}(S_i) = \frac{\mu_F(S_i)}{\mu_S(S_i) + \mu_F(S_i)}, S_i \in U.$$

For $S_i, S_j \in U$, the profust interval reliability over a time interval $[t_0, t]$ is defined as [14]

$$\begin{aligned} R(t_0, t) &= P\{T_{SF} \text{ does not occur during } [t_0, t]\} \\ &= 1 - P\{T_{SF} \text{ occurs during } [t_0, t]\} \\ &= 1 - \sum_{i=1}^n \sum_{j=1}^n \mu_{T_{SF}}(m_{ij}) \cdot p_{ij}(t_0, t). \end{aligned}$$

where $p_{ij}(t_0, t)$ is transition probability from state S_i to state S_j over an time interval $[t_0, t]$. The profust reliability is defined as [14]

$$R(t) = R(0, t).$$

For the purpose of real-time performance monitoring, reference [22] proposed a new profust reliability definition. Define fuzzy events A is $\{T_{SF} \text{ does not}$

occur during time interval $[t_0, t]$, and B is {The system performance is in fuzzy success state at initial time t_0 }. Then, For $S_i, S_j \in U$, and a time interval $[t_0, t]$, the profust reliability $R(t)$ is defined as (1) at the bottom of the page [22]. In (1), $\varphi_{S_i}(t_0)$ is the health state probability of state S_i at time t_0 . Here, the time interval $[t_0, t]$ can be viewed as a sliding calculation interval during the real-time reliability calculation.

Remark 1. The physical meaning of the profust reliability at time t is the probability that no further health status deterioration occurs during a time interval $[t_0, t]$. Thus, the profust reliability $R(t)$ defined by (1) has its ability to accurately track the performance variation, which can be viewed as a definition of the performance reliability (*i.e.*, the concept of PPR in this paper). However, in [22], the transition probability $p_{ij}(t_0, t)$ is dynamically acquired based on statistical results, which is inaccurate and insufficient to reflect the performance degradation without abundant data samples. Furthermore, the PPR’s prediction is based on the update of the transition probability $p_{ij}(t_0, t)$, which is somewhat complex to implement in practice. To improve PPR’s calculation accuracy and reduce algorithm complexity, a modified PPR algorithm based on (1) is proposed in the following.

Before developing further, an assumption is introduced. Without loss of generality, let $\mu_F(S_n) \leq \mu_F(S_{n-1}) \leq \dots \leq \mu_F(S_2) \leq \mu_F(S_1)$.

Assumption 1. For the transition probability $p_{ij}(t_0, t)$, it satisfies that

$$p_{ij}(t_0, t) = 0, \text{ if } j > i$$

where $i, j \in \{1, 2, \dots, n\}$.

Remark 2. Assumption 1 implies that system state transitions will not occur from a worse state to a better state during its whole lifecycle without maintenance actions. Under this assumption, a theorem is stated to present the modified PPR algorithm in the following.

Theorem 1. Under Assumption 1, suppose that the system performance is in state S_i at time t_0 with the probability $\varphi_{S_i}(t_0)$, where

$$\begin{cases} \varphi_{S_i}(t_0) \geq 0 & S_i \in U \\ \sum_{i=1}^n \varphi_{S_i}(t_0) = 1 \end{cases}$$

Then, the PPR is calculated as (2) at the bottom of the page.

Proof. See the Appendix A.

Remark 3. Equation (2) is a modified version of (1), where the item of transition probability among system’s multi-states in (1) is replaced with the real-time distribution of system’s health status in (2). Compared with the previous algorithm, the modified one improves the PPR calculation accuracy by avoiding the statistical calculation of transition probabilities. Furthermore, the PPR prediction is easier to be implemented in practice by the modified PPR algorithm.

During the process of real-time PPR calculation, the system performance might be in a fully successful status, or operate in a degraded level at the start point t_0 of the calculation interval. Theorem 1 covers all situations that might appear at the beginning of the evaluation interval. Based on Theorem 1, two corollaries are further obtained.

Corollary 1. Under Assumption 1, suppose that the system performance is in state S_n at time t_0 ,

$$\varphi_{S_i}(t_0) = \begin{cases} 0 & i = 1, 2, \dots, n - 1 \\ 1 & i = n \end{cases}$$

Then, the PPR is

$$R(t) = \mu_S(S_n) \cdot \left[1 - \left(\sum_{j=1}^{n-1} \mu_{TSF}(m_{nj}) \cdot \varphi_{S_j}(t) \right) \right]$$

$$\begin{aligned} R(t) &= P(A | B) \cdot P(B) = 1 - P(\bar{A} | B) \cdot P(B) - P(\bar{B}) \\ &= 1 - \left[\sum_{i=1}^n \sum_{j=1}^n \mu_{TSF}(m_{ij}) \cdot p_{ij}(t_0, t) \right] \cdot \left[\sum_{i=1}^n \mu_S(S_i) \cdot \varphi_{S_i}(t_0) \right] - \sum_{i=1}^n \mu_F(S_i) \cdot \varphi_{S_i}(t_0). \end{aligned} \tag{1}$$

$$R(t) = 1 - \left\{ \sum_{i=2}^n \varphi_{S_i}(t_0) \cdot \left[\sum_{j=1}^{i-1} \mu_{TSF}(m_{ij}) \cdot \varphi_{S_j}(t) \right] \right\} \cdot \left[\sum_{i=1}^n \mu_S(S_i) \cdot \varphi_{S_i}(t_0) \right] - \sum_{i=1}^n \mu_F(S_i) \cdot \varphi_{S_i}(t_0). \tag{2}$$

Furthermore, if $\mu_F(S_n) = 0$, the PPR is

$$R(t) = \sum_{j=1}^n \mu_S(S_j) \varphi_{S_j}(t). \quad (3)$$

proof. See the Appendix B.

Remark 4. The premise of Corollary 1 is that the system performance must be fully healthy at time t_0 , and then the PPR can be only calculated with the distribution of system's health status at time t .

Corollary 2. Under Assumption 1, suppose that the system performance is in a specific state S_q at time t_0 for certain,

$$\varphi_{S_i}(t_0) = \begin{cases} 0 & i = 1, 2, \dots, n, i \neq q \\ 1 & i = q \end{cases},$$

and the system performance is in a specific state S_j at time t for certain,

$$\varphi_{S_i}(t) = \begin{cases} 0 & i = 1, 2, \dots, n, i \neq j \\ 1 & i = j \end{cases}.$$

Then, the PPR is

$$R(t) = \mu_S(S_q) \cdot (1 - \mu_{TSF}(m_{qj})). \quad (4)$$

Proof. See the Appendix C.

Remark 5. Corollary 2 satisfies the situation that the system status is definitely determined during the PPR calculation process. Both the two corollaries are the simplification of Theorem 1, and any of them can be selected to perform the PPR calculation according to practical engineering demands.

3. Performance evaluation and prediction of dynamic system

For the purpose of performing the modified PPR algorithm on engineering applications, a process of performance evaluation and prediction for dynamic systems is comprehensively presented.

3.1. Problem formulation

The following nonlinear discrete time dynamic system is considered in this part,

$$\begin{cases} \mathbf{x}(t_k) = \mathbf{F}(\mathbf{x}(t_{k-1}), \mathbf{u}(t_{k-1})) + \mathbf{w}(t_k) \\ \mathbf{y}(t_k) = \mathbf{h}(\mathbf{x}(t_k)) + \mathbf{v}(t_k) \end{cases}, \quad (5)$$

where $\mathbf{x} \in \mathbb{R}^{N \times 1}$ is the vector of SSVs; $\mathbf{F}(\mathbf{x}(t_{k-1}), \mathbf{u}(t_{k-1}))$ and $\mathbf{h}(\mathbf{x}(t_k))$ are nonlinear functions; $\mathbf{w}(t_k)$ and $\mathbf{v}(t_k)$ are the system noise and measurement noise, respectively.

Assumption 2. The system noise $\mathbf{w}(t_k)$ and measurement noise $\mathbf{v}(t_k)$ satisfy that

$$\begin{cases} \mathbf{w}(t_k) \sim \mathcal{N}(0, \mathbf{Q}_w), \mathbf{v}(t_k) \sim \mathcal{N}(0, \mathbf{Q}_v), \forall k \\ \text{cov}[\mathbf{w}(t_k), \mathbf{v}(t_j)] = E[\mathbf{w}(t_k) \mathbf{v}^T(t_j)] = 0, \forall k, j \end{cases}$$

where \mathbf{Q}_w and \mathbf{Q}_v are the covariance matrices.

Remark 6. Various dynamic systems in practice can be represented in the form of (5). Thus, the performance evaluation and prediction method based on (5) is without loss of generality.

Considering the tight connection between the system performance and the system reliability, the main objective of this part is to evaluate and predict the performance reliability of dynamic systems based on the modified PPR algorithm as shown in Section 2. In practice, the performance of a dynamic system will be reflected in the variation of SSVs. Therefore, a definition of the performance reliability of dynamic systems should be given on this basis. In this paper, for system (5), the performance reliability at time t_k is defined as

$$\begin{aligned} R_{\text{sys}}(t_k) &= \Psi(R_{x_1}(t_k), \dots, R_{x_i}(t_k), \dots, R_{x_N}(t_k)), \quad (6) \end{aligned}$$

where x_i is the i th element of \mathbf{x} ; $R_{x_i}(t_k)$ is the performance reliability of the SSV x_i at time t_k ; Ψ is a known function reflecting the relation between the system performance and the performance of SSVs. In practice, Ψ can be determined according to practical engineering demands.

Remark 7. Equation (6) indicates that the performance reliability of a dynamic system is calculated with the performance reliability of each SSV. For a specific component x_m in \mathbf{x} , we can define its performance reliability with the PPR concept, and calculate its PPR by Theorem 1 as shown in (7) at the bottom of the next page.

The PPR of other SSVs in \mathbf{x} can be also calculated according to Theorem 1, which has a similar form as presented in (7). It indicates that the SSV's

performance at a specific time index can be evaluated by its health status variation in a time interval.

So far, the main task in this part is to calculate the PPR of each SSV. In (7), PPR is mainly defined with the real-time health status distribution, which cannot be directly acquired from the unknown value of a SSV. Thus, the main difficulty in this process is how to obtain the real-time distribution of the SSV, and further the real-time distribution of SSV's health status. In this paper, EKF and the exponential smoothing method are employed to estimate and predict the real-time distribution of SSVs, respectively, where both the mean values and error variances of SSVs are obtained. Then, the real-time health status distribution of each SSV is obtained based on the obtained SSV's distribution and its health status classification.

3.2. Performance evaluation of dynamic systems

To evaluate the performance of the dynamic system presented in (5), following steps are required as shown in Fig. 1.

In the presented procedure, the PPR of each SSV is firstly calculated, and then the performance of the dynamic system is evaluated according to (6). For the process of PPR calculation of a single SSV, EKF is firstly employed to estimate the real-time distribution of the SSV, where both the mean value and error variance of the SSV are obtained. Then, considering the true but unknown value of the SSV at a specific time index conforms to a normal distribution, the real-time health status distribution of the SSV can be obtained based on the estimation results of the SSV and its health status classification. On this basis, the PPR of the studied SSV is calculated in real time with the proposed PPR algorithm presented in Section 2. Here, a specific SSV $x_m \in \mathbf{x}$ is illustrated here to present the process of calculating the PPR of a single SSV.

3.2.1. Real-time distribution estimation of SSV

In order to acquire the estimate of the system state vector \mathbf{x} of (5), EKF is implemented here. Equation (8) gives the main steps of EKF,

$$\begin{cases} \hat{\mathbf{x}}(t_k | t_{k-1}) = \mathbf{F}(\hat{\mathbf{x}}(t_{k-1} | t_{k-1}), \mathbf{u}(t_{k-1})) \\ \boldsymbol{\Sigma}(t_k | t_{k-1}) = \mathbf{A}_{k-1} \boldsymbol{\Sigma}(t_{k-1} | t_{k-1}) \mathbf{A}_{k-1}^T + \mathbf{Q}_w \\ \mathbf{K}(t_k) = \boldsymbol{\Sigma}(t_k | t_{k-1}) \mathbf{C}_k^T \\ \cdot [\mathbf{C}_k \boldsymbol{\Sigma}(t_k | t_{k-1}) \mathbf{C}_k^T + \mathbf{Q}_v]^{-1} \\ \hat{\mathbf{x}}(t_k | t_k) = \hat{\mathbf{x}}(t_k | t_{k-1}) + \mathbf{K}(t_k) \\ \cdot [\mathbf{y}(t_k) - \mathbf{h}(\hat{\mathbf{x}}(t_k | t_{k-1}))] \\ \boldsymbol{\Sigma}(t_k | t_k) = [\mathbf{I} - \mathbf{K}(t_k) \mathbf{C}_k] \boldsymbol{\Sigma}(t_k | t_{k-1}) \end{cases}, \quad (8)$$

where $\boldsymbol{\Sigma}$ is the error covariance matrix; \mathbf{K} is the Kalman gain; \mathbf{A}_{k-1} and \mathbf{C}_k are the linearized matrices computed as

$$\begin{cases} \mathbf{A}_{k-1} = \frac{\partial \mathbf{F}}{\partial \mathbf{x}} \Big|_{\hat{\mathbf{x}}(t_{k-1}|t_{k-1}), \mathbf{u}(t_{k-1})} \\ \mathbf{C}_k = \frac{\partial \mathbf{h}}{\partial \mathbf{x}} \Big|_{\hat{\mathbf{x}}(t_k|t_{k-1})} \end{cases}.$$

According to the results of EKF, it is obtained that

$$\begin{cases} E[\mathbf{x}(t_k)] = \hat{\mathbf{x}}(t_k | t_k) \\ E\left\{[\mathbf{x}(t_k) - \hat{\mathbf{x}}(t_k | t_k)][\mathbf{x}(t_k) - \hat{\mathbf{x}}(t_k | t_k)]^T\right\} \\ = \boldsymbol{\Sigma}(t_k | t_k) \end{cases}.$$

Under Assumption 2, it can be derived from [23] that

$$\mathbf{x}(t_k) \sim \mathcal{N}(\hat{\mathbf{x}}(t_k | t_k), \boldsymbol{\Sigma}(t_k | t_k)). \quad (9)$$

Then, for the studied SSV x_m ,

$$x_m(t_k) \sim \mathcal{N}(\hat{x}_m(t_k | t_k), \Sigma_{(m,m)}(t_k | t_k)), \quad (10)$$

where $\Sigma_{(m,m)}(t_k | t_k)$ is the m th diagonal element of $\boldsymbol{\Sigma}(t_k | t_k)$.

3.2.2. Health status classification of SSV

Suppose $x_m \in [a, b]$, the health status of SSV can be classified into discrete health states according to the value of x_m ,

$$S_i = \{x_m | a_i < x_m \leq a_{i-1}\}, \quad (11)$$

where

$$a_i = a + (i - 1) \cdot \delta, i = 2, 3, \dots, n, \delta = \frac{b - a}{n - 1}, \quad (12)$$

$$\begin{aligned} R_{x_m}(t_k) = & 1 - \left\{ \sum_{i=2}^n \varphi_{x_m, S_i}(t_0) \cdot \left[\sum_{j=1}^{i-1} \mu_{TSF}(m_{ij}) \cdot \varphi_{x_m, S_j}(t_k) \right] \right\} \cdot \left[\sum_{i=1}^n \mu_S(S_i) \cdot \varphi_{x_m, S_i}(t_0) \right] \\ & - \sum_{i=1}^n \mu_F(S_i) \cdot \varphi_{x_m, S_i}(t_0). \end{aligned} \quad (7)$$

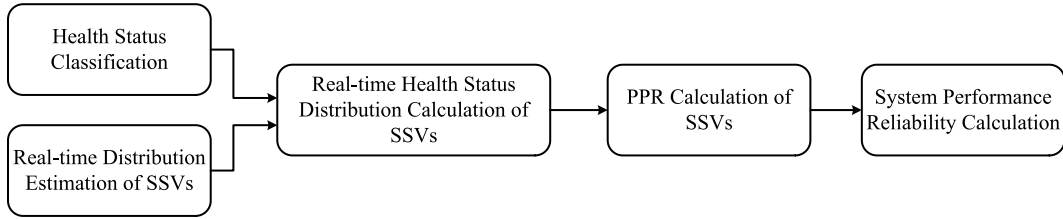


Fig. 1. Procedure of the system performance evaluation.

and

$$S_1 = \{x_m \mid x_m \notin [a, b]\}. \tag{13}$$

Remark 8. The emphasis of the health status classification is to satisfy $\mu_F(S_n) \leq \mu_F(S_{n-1}) \leq \dots \leq \mu_F(S_2) \leq \mu_F(S_1)$. Thus, the classification principle above may need to adjust according to SSV's real data and the selected membership function.

3.2.3. Real-time health status distribution calculation of SSV

From the former two steps, the real-time distribution of $x_m(t_k)$, and its health status classification are obtained. On this basis, its real-time health status distribution is obtained in the following.

For $i = 2, 3, \dots, n$, combining (10), (11), and (12), Equation (14) at the bottom of the page can be obtained, where Φ is denoted as the cumulative distribution function of standard normal distribution [24]. For the case $i = 1$,

$$\begin{aligned} \varphi_{x_m, S_1}(t_k) &= P\{x_m(t_k | t_k) \notin [a, b]\} \\ &= 1 - P\{a \leq x_m(t_k | t_k) \leq b\} \\ &= 1 - G\left(b, a, \hat{x}_m(t_k | t_k), \sqrt{\Sigma_{(m,m)}(t_k | t_k)}\right). \end{aligned}$$

To sum up, Equation (15) at the bottom of the page can be obtained.

3.2.4. PPR calculation of SSV

Following the above steps, Equation (2) can be directly employed to calculate the PPR of x_m . Note that the PPR of other SSVs can be also calculated following the above steps.

Remark 9. Equation (2) in Theorem 1 can be used for the PPR evaluation of a single SSV. In particular, there exist two noteworthy cases. For one thing, if the SSV's performance can be definitely determined to be fully successful at the start time t_0 of the evaluation interval, Equation (2) can be replaced with (3) in Corollary 1 to calculate PPR for simplicity. For another, if $\Sigma_{(m,m)}(t_k | t_k)$ in (10) is small enough, it can be approximately considered that $x_m(t_k) \doteq \hat{x}_m(t_k | t_k)$, which means that the SSV's health status can be definitely determined without importing probability distribution. In this situation, Equation (2) can be replaced with (4) in Corollary 2 for simplicity.

3.2.5. System performance reliability calculation

Following the PPR algorithm of a single SSV, the PPR calculation results of all SSVs in (5) are obtained in real time as

$$\begin{aligned} \varphi_{x_m, S_i}(t_k) &= P\{a_i < x_m(t_k | t_k) \leq a_{i-1}\} \\ &= P\left\{ \frac{a_i - \hat{x}_m(t_k | t_k)}{\sqrt{\Sigma_{(m,m)}(t_k | t_k)}} < \frac{x_m(t_k | t_k) - \hat{x}_m(t_k | t_k)}{\sqrt{\Sigma_{(m,m)}(t_k | t_k)}} \leq \frac{a_{i-1} - \hat{x}_m(t_k | t_k)}{\sqrt{\Sigma_{(m,m)}(t_k | t_k)}} \right\} \\ &= \Phi\left(\frac{a_{i-1} - \hat{x}_m(t_k | t_k)}{\sqrt{\Sigma_{(m,m)}(t_k | t_k)}}\right) - \Phi\left(\frac{a_i - \hat{x}_m(t_k | t_k)}{\sqrt{\Sigma_{(m,m)}(t_k | t_k)}}\right) \\ &\triangleq G\left(a_{i-1}, a_i, \hat{x}_m(t_k | t_k), \sqrt{\Sigma_{(m,m)}(t_k | t_k)}\right), \end{aligned} \tag{14}$$

$$\varphi_{x_m, S_i}(t_k) = \begin{cases} 1 - G\left(b, a, \hat{x}_m(t_k | t_k), \sqrt{\Sigma_{(m,m)}(t_k | t_k)}\right) & i = 1 \\ G\left(a_{i-1}, a_i, \hat{x}_m(t_k | t_k), \sqrt{\Sigma_{(m,m)}(t_k | t_k)}\right) & i = 2, 3, \dots, n \end{cases} \tag{15}$$

Table 1
Procedure of the system performance evaluation

| | |
|---------|--|
| Step 1. | For a single SSV x_m , estimate its distribution by EKF according to (8), where the mean and error variance are obtained. For the time t_0 and t_k , it is obtained that $x_m(t_0) \sim \mathcal{N}(\hat{x}_m(t_0), \Sigma_{(m,m)}(t_0))$, $x_m(t_k) \sim \mathcal{N}(\hat{x}_m(t_k), \Sigma_{(m,m)}(t_k))$. |
| Step 2. | Classify the health status of x_m in terms of its value according to (11–13). Then, n health states of the SSV x_m are acquired as $U = \{S_1, S_2, \dots, S_n\}$. |
| Step 3. | Based on the two former steps, calculate the health status distribution at time t_0 and t_k according to (15), written as $\varphi_{x_m, S_i}(t_0)$ and $\varphi_{x_m, S_i}(t_k)$. |
| Step 4. | Calculate the PPR of x_m at time t_k by <i>Theorem 1</i> , or <i>Corollaries 1&2</i> . |
| Step 5. | Repeating steps 1-4, calculate the PPR of each SSV at time t_k as $\{R_{x_1}(t_k), \dots, R_{x_m}(t_k), \dots, R_{x_N}(t_k)\}$. |
| Step 6. | Based on results from step 5, calculate the system performance reliability $R_{sys}(t_k)$ by (6). |

$$\{R_{x_1}(t_k), \dots, R_{x_m}(t_k), \dots, R_{x_N}(t_k)\}.$$

Then, the system performance reliability is calculated according to (6).

For a specific evaluation interval $[t_0, t_k]$, the procedure of the system performance evaluation at time t_k of the dynamic system (5) with performing the modified PPR algorithm is summarized as shown in Table 1.

3.3. Performance prediction of dynamic systems

The process of the system performance prediction is similar to the evaluation process presented above. The PPR of each SSV is firstly predicted, and then the system performance is determined with the predicted value of the system performance reliability.

Here, the SSV x_m is further cited as an example. In order to predict the PPR of x_m at a future time index t_{k+l} , the distribution of x_m should be firstly predicted as

$$\hat{x}_m(t_{k+l}) \sim \mathcal{N}(\hat{x}_m(t_{k+l} | t_k), \hat{\Sigma}_{(m,m)}(t_{k+l} | t_k)), \tag{16}$$

where l is the prediction step. Then, the classification of the health status and its distribution calculation are similarly performed as that in the performance evaluation process. Finally, the PPR of x_m at time t_{k+l} is predicted in (17) at the bottom of the page, where the probability component $\varphi_{x_m, S_i}(\cdot)$ is obtained by (15).

By following the above steps, for the system (5), the PPR prediction result of all SSVs can be obtained.

Then, the system performance reliability at time t_{k+l} is predicted as shown in (18) at the bottom of the next page.

3.3.1. Real-time prediction method of SSV's distribution

In the PPR prediction process of a single SSV, the most critical part is to accurately predict the distribution of the SSV. Here, multiple methods can be employed to predict the distribution of the SSV as stated in (16). The Holt-Winters double exponential smoothing [3] is implemented here as an alternative method to perform short-term prediction. For the SSV x_m , given the results from EKF in (9), the smoothed value of SSV is computed as

$$\begin{cases} u_k = \alpha \hat{x}_m(t_k | t_k) + (1 - \alpha)(u_{k-1} + v_{k-1}) \\ v_k = \beta(u_k - u_{k-1}) + (1 - \beta)v_{k-1} \end{cases}, \tag{19}$$

where $\alpha, \beta \in (0, 1)$ are the smoothing parameters. The initial values of u_k, v_k are

$$u_1 = \hat{x}_m(t_1 | t_1), u_2 = \hat{x}_m(t_2 | t_2),$$

and

$$v_2 = u_2 - u_1.$$

On the basis of (19), the predicted value of x_m is computed as

$$\hat{x}_m(t_{k+l} | t_k) = u_k + v_k \cdot l.$$

$$\begin{aligned} &\hat{R}_{x_m}(t_{k+l} | t_k) \\ &= 1 - \left\{ \sum_{i=2}^n \varphi_{x_m, S_i}(t_k) \cdot \left[\sum_{j=1}^{i-1} \mu_{TSF}(m_{ij}) \cdot \hat{\varphi}_{x_m, S_j}(t_{k+l}) \right] \right\} \cdot \left[\sum_{i=1}^n \mu_S(S_i) \cdot \hat{\varphi}_{x_m, S_i}(t_k) \right] \\ &\quad - \sum_{i=1}^n \mu_F(S_i) \cdot \hat{\varphi}_{x_m, S_i}(t_k), \end{aligned} \tag{17}$$

Table 2
Procedure of the system performance prediction

| | |
|---------|---|
| Step 1. | For a single SSV x_m , the estimated distribution of at time t_k has already obtained by EKF. For the time t_{k+l} , predict the distribution $\hat{x}_m(t_{k+l})$ by methods such as the exponential smoothing method. |
| Step 2. | The health status classification of x_m remains same as performed in the evaluation process. |
| Step 3. | The health status distribution $\varphi_{x_m, S_j}(t_k)$ of x_m at time t_k is already obtained in the evaluation process. Also, based on the two former steps, calculate the predicted health status distribution $\hat{\varphi}_{x_m, S_j}(t_{k+l})$ of x_m at time t_{k+l} . |
| Step 4. | Calculate the predicted PPR of x_m at time t_{k+l} by <i>Theorem 1</i> , or <i>Corollaries 1&2</i> . |
| Step 5. | Repeating steps 1-4, predict the PPR of each SSV at time t_{k+l} as $\{\hat{R}_{x_1}(t_{k+l} t_k), \dots, \hat{R}_{x_m}(t_{k+l} t_k), \dots, \hat{R}_{x_N}(t_{k+l} t_k)\}$. |
| Step 6. | Based on results from step 5, calculate the system performance reliability $\hat{R}_{sys}(t_{k+l} t_k)$ by (18). |

According to [3], the l -step prediction error variances of the proposed method can be estimated as

$$\hat{\sigma}^2(l) = [1 + \alpha^2(l - 1) + (1 + \beta + l\beta^2(2l - 1)/6)] \cdot s^2(1),$$

where $s^2(1)$ is the mean square error of 1-step prediction. Thus, Equation (16) becomes

$$\hat{x}_m(t_{k+l}) \sim \mathcal{N}(u_k + v_k \cdot l, \hat{\sigma}^2(l)).$$

Then, Equation (17) can be directly used to achieve PPR prediction, where

$$\varphi_{x_m, S_j}(t_{k+l}) = \begin{cases} 1 - G(b, a, u_k + v_k \cdot l, \hat{\sigma}(l)) & j = 1 \\ G(a_{j-1}, a_j, u_k + v_k \cdot l, \hat{\sigma}(l)) & j = 2, \dots, n \end{cases}$$

For a specific prediction interval $[t_k, t_{k+l}]$, the procedure of the system performance prediction at time t_{k+l} with performing the modified PPR algorithm is summarized as shown in Table 2.

Remark 10. The presented PPR-based performance prediction method is a general framework, where the Holt-Winters double exponential smoothing is just an alternative method to perform short-term prediction of the SSV's distribution. In practice, other effective prediction methods can be employed to serve for the PPR-based system performance prediction framework.

4. Simulation

In this section, a simulation of a quadrotor with partial loss of actuator effectiveness is presented to validate the availability and effectiveness of the

proposed PPR-based performance evaluation and prediction method.

4.1. Quadrotor model

Scholars have studied the dynamics of quadrotor [25–29]. Equation (20) presents a general dynamic model:

$$\begin{aligned} \dot{x} &= v_x \\ \dot{y} &= v_y \\ \dot{z} &= v_z \\ \dot{v}_x &= u_z (\cos \phi \sin \theta \cos \psi + \sin \phi \sin \psi) / m \\ \dot{v}_y &= u_z (\cos \phi \sin \theta \sin \psi - \sin \phi \cos \psi) / m \\ \dot{v}_z &= u_z \cos \phi \cos \theta / m - g \\ \dot{\phi} &= p + \tan \theta (r \cos \phi + q \sin \phi) \\ \dot{\theta} &= q \cos \phi - r \sin \phi \\ \dot{\psi} &= \sec \theta (r \cos \phi + q \sin \phi) \\ \dot{p} &= (J_y - J_z) r q / J_x + u_\phi / J_x \\ \dot{q} &= (J_z - J_x) p r / J_y + u_\theta / J_y \\ \dot{r} &= (J_x - J_y) p q / J_z + u_\psi / J_z \end{aligned} \tag{20}$$

$$\underbrace{\dot{X}} = F_q(X, u)$$

where x, y, z are the position components in the earth-fixed frame; v_x, v_y, v_z are the velocity components in the earth-fixed frame; ϕ, θ, ψ are the angles of roll, pitch, and yaw, respectively; p, q, r are the angular velocity of ϕ, θ, ψ ; J_x, J_y, J_z are the moments of inertia along x, y, z directions, respectively; u_z is the total lift generated by rotors, and u_ϕ, u_θ, u_ψ are the torques along the directions of the ϕ, θ, ψ angles, respectively. The control input $u = [u_z, u_\phi, u_\theta, u_\psi]^T$ is transferred by the lift of four rotors $f = [f_1, f_2, f_3, f_4]^T$, satisfying

$$\hat{R}_{sys}(t_{k+l} | t_k) = \Psi(\hat{R}_{x_1}(t_{k+l} | t_k), \dots, \hat{R}_{x_m}(t_{k+l} | t_k), \dots, \hat{R}_{x_N}(t_{k+l} | t_k)). \tag{18}$$

$$\mathbf{u} = \mathbf{H}\mathbf{f}, \quad (21)$$

where the transfer matrix \mathbf{H} (also known as control effectiveness matrix) is

$$\mathbf{H} = \begin{bmatrix} \eta_1 & \eta_2 & \eta_3 & \eta_4 \\ 0 & \eta_2 d_2 & 0 & -\eta_4 d_4 \\ \eta_1 d_1 & 0 & -\eta_3 d_3 & 0 \\ -\eta_1 \lambda_1 & \eta_2 \lambda_2 & -\eta_3 \lambda_3 & \eta_4 \lambda_4 \end{bmatrix}, \quad (22)$$

where d_i is the distance from the center of the i th rotor to the center of mass; λ_i is the ratio between the torque and the lift of the i th rotor; the parameter $\eta_i \in [0, 1]$ represents the effectiveness of the i th rotor (as well as the control effectiveness of the i th actuator). The value $\eta_i = 1$ means the i th rotor is in a normal condition; The value $\eta_i = 0$ means a complete loss of effectiveness of the i th rotor.

To obtain the discrete dynamic model of the presented quadrotor, Equation (20) is discretized through the Euler method [30]. Considering the system noise and measurement noise, the discrete model is written as

$$\begin{cases} \mathbf{X}(t_k) = \mathbf{X}(t_{k-1}) + T\mathbf{F}_q(\mathbf{X}(t_{k-1}), \mathbf{u}(t_{k-1})) \\ + \mathbf{\Gamma}\mathbf{w}(t_k) \\ \mathbf{Y}(t_k) = \mathbf{X}(t_k) + \mathbf{v}(t_k) \end{cases},$$

where the noise driven matrix $\mathbf{\Gamma} = \text{diag}\{0, 0, 0, 1, 1, 1, 0, 0, 0, 1, 1, 1\}$. Here, all the SSVs of the quadrotor are directly measured.

The parameters of the studied quadrotor is shown in Table 3.

In this simulation, the quadrotor is required to perform a persistent surveillance mission. It is desired that the quadrotor hovers at a height of 10m, while the attitude angles remains stable.

4.2. Quadrotor's performance evaluation and prediction

In the studied hovering maneuver, the roll, pitch, yaw angle, and the position component in z -direction

Table 3
Quadrotor model parameters

| | |
|--|--|
| m | 1.535 kg |
| J_x, J_y, J_z | 0.0411, 0.0478, 0.0599 kg · m ² |
| g | 9.8 m/s ² |
| L_1, L_2, L_3, L_4 | 0.28 m |
| $\lambda_1, \lambda_2, \lambda_3, \lambda_4$ | 1 |
| $\mathbf{Q}_w, \mathbf{Q}_v$ | $5 \times 10^{-5} I_{12}$ |
| T | 0.1 s |

can totally reflect the quadrotor's performance. In this case, according to (6), the quadrotor's performance reliability is given with two alternative forms as

$$R_{\text{sys}1} = R_\phi \cdot R_\theta \cdot R_\psi \cdot R_z \quad (23)$$

and

$$R_{\text{sys}2} = w_\phi R_\phi + w_\theta R_\theta + w_\psi R_\psi + w_z R_z, \quad (24)$$

where $R_\phi, R_\theta, R_\psi, R_z$ are the PPR of ϕ, θ, ψ, z , respectively; $w_\phi, w_\theta, w_\psi, w_z$ are the corresponding weights fulfilling the condition that $\sum w = 1$. In practice, the weights should be determined according to historical data analysis, and engineering requirements. Note that both $R_{\text{sys}1}$ and $R_{\text{sys}2}$ can represent quadrotor's performance reliability. Equation (23) assumes that the SSVs have a serial relation to reflect the quadrotor's performance. It deems that a single SSV's performance can totally influence the quadrotor's performance. For (24), the quadrotor's performance is calculated with the weighted sum of SSV's performance. This means that a single SSV's performance with a certain weight. For simplicity, let $w_\phi = w_\theta = w_z = 0.3$, and $w_\psi = 0.1$ in this simulation. This is because ϕ, θ, z are more important than ψ to characterize the system performance for a hovering quadrotor.

Considering the hovering characteristics, trapezoidal membership functions are selected as the fuzzy success function of the SSVs. The functions of $\mu_S(\phi), \mu_S(\theta), \mu_S(\psi), \mu_S(z)$, and the corresponding health status classification are presented in Appendix D.

For the performance evaluation and prediction of the quadrotor, three scenarios are presented here to validate the effectiveness of the proposed PPR-based method, including a fault-free scenario, a fixed-fault scenario, and a gradual-degradation scenario. In all the scenarios, the simulation step T is set to be 0.1s, and the total simulation time is 80s.

4.2.1. Fault-free scenario

In this part, the rotors of quadrotors are completely healthy. Thus, in (22), we have

$$\begin{aligned} \eta_1(t_k) &= \eta_2(t_k) = \eta_3(t_k) \\ &= \eta_4(t_k) = 1, \quad t_k \in [0, 80]. \end{aligned}$$

Figure 2 shows the variations of the SSVs ϕ, θ, ψ, z estimated by EKF. With performing the proposed PPR-based algorithm, the system performance is

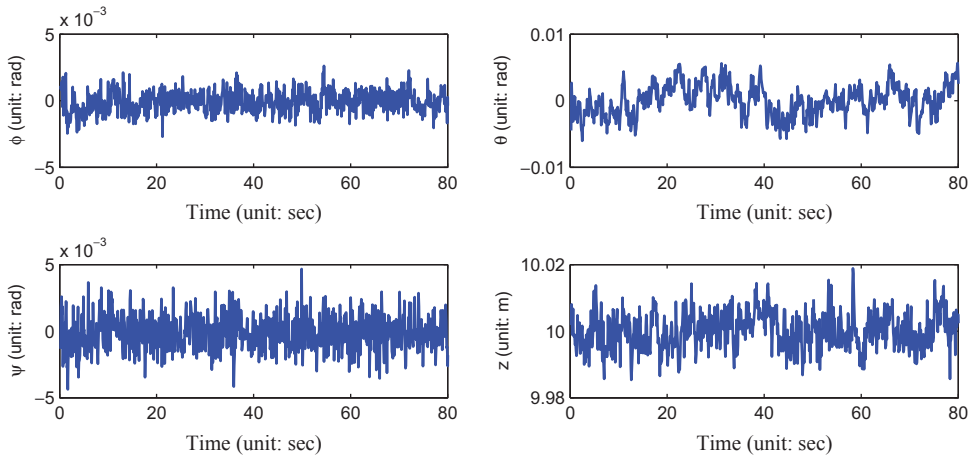


Fig. 2. Variations of ϕ, θ, ψ, z in fault-free scenario. It is demonstrated that the value of $[\phi, \theta, \psi, z]^T$ is relatively stable and fluctuates around the value $[0, 0, 0, 10]^T$ in a small range, which satisfies the requirement of hovering maneuver.

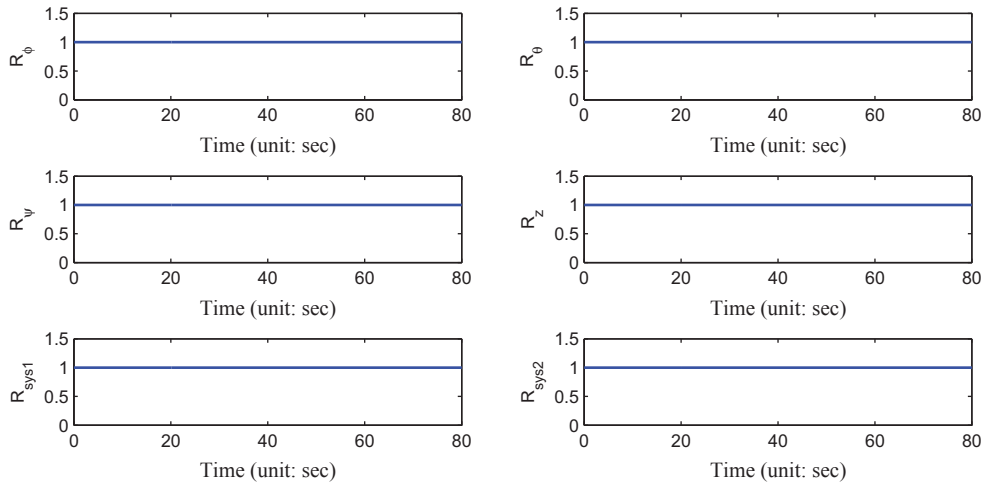


Fig. 3. PPR evaluation result in fault-free scenario. The calculated PPRs of ϕ, θ, ψ, z are steadily equal to 1, and the PPR of the quadrotor is also equal to 1.

evaluated per 0.2 second ($[t_0, t_k]$ in *Theorem 1*) as depicted in Fig. 3.

4.2.2. Fixed-fault scenario

In this part, the two of four rotors of quadrotors confront to fixed partial loss of effectiveness. In (22), for $t_k \in [0, 30]$, let

$$\eta_1(t_k) = \eta_2(t_k) = \eta_3(t_k) = \eta_4(t_k) = 1$$

and for $t_k \in (30, 80]$, let

$$\begin{aligned} \eta_1(t_k) &= \eta_4(t_k) = 1 \\ \eta_2(t_k) &= \eta_3(t_k) = 0.85 \end{aligned}$$

Such kind of fault may happen due to severe weather conditions damaging the rotors or physical collision with obstacles [25].

Under this scenario, Fig. 4 shows the variations of the SSVs ϕ, θ, ψ, z estimated by EKF. With performing the proposed PPR-based algorithm, the system performance is also evaluated per 0.2 second as depicted in Fig. 5. It should be noted that the PPRs of θ and ψ keep at 1. That is because although there also exists deviation of the variation of θ and ψ , the deviation is tolerant according to the configuration of the employed membership functions. If it is required to improve sensitivity to the emerged fault, thresholds of membership

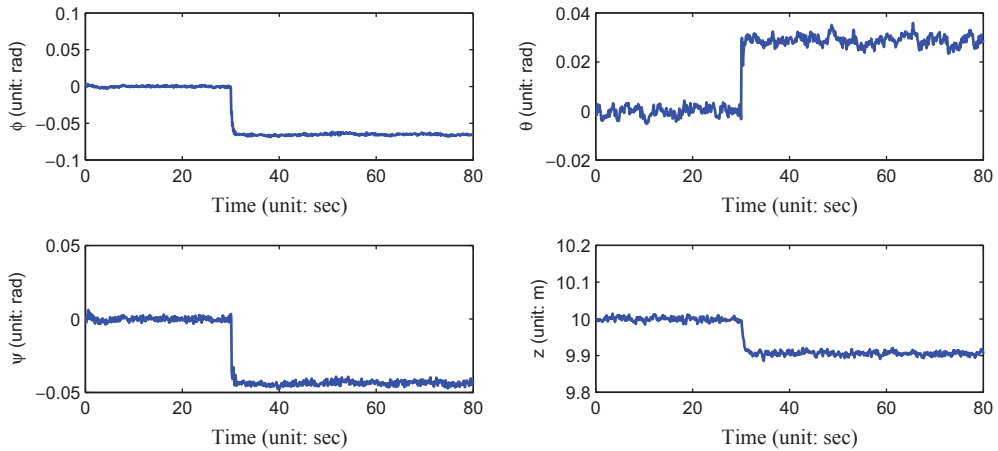


Fig. 4. Variations of ϕ, θ, ψ, z in fixed-fault scenario. It is shown that the value of $[\phi, \theta, \psi, z]^T$ is relatively stable during the interval $[0, 30]$. After that, a certain deviation of ϕ, θ, ψ, z is occurred due to fixed partial loss of actuator effectiveness.

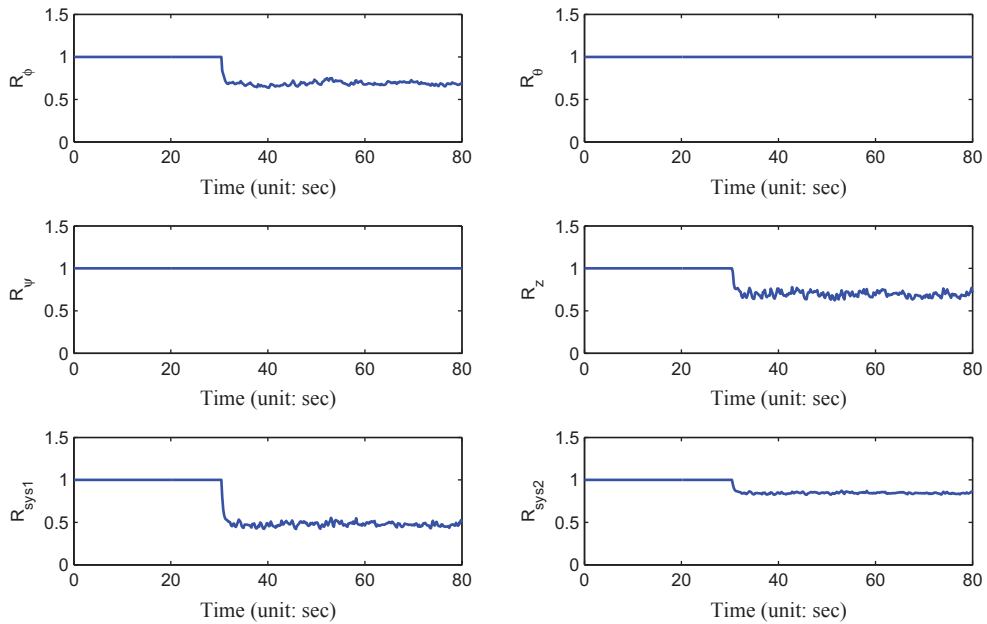


Fig. 5. PPR evaluation result in fixed-fault scenario. The calculated PPRs of ϕ, z are suddenly decreased at $t = 30s$, and the quadrotor's performance also deteriorates as indicated by the quadrotor's PPR.

functions might be adjusted according to engineering requirements.

4.2.3. Gradual-degradation scenario

In this part, the two of four rotors of quadrotors confront to gradual-degradation of effectiveness. In (22), this phenomenon is addressed as follows:

$$\eta_1(t_k) = \eta_4(t_k) = 1, \quad t_k \in [0, 80],$$

$$\eta_2(t_k) = \begin{cases} 1 & t_k \in [0, 10] \\ \eta_2(t_{k-T}) - 5 \times 10^{-4} & t_k \in (10, 80] \end{cases},$$

$$\eta_3(t_k) = \begin{cases} 1 & t_k \in [0, 10] \\ \eta_3(t_{k-T}) - 5 \times 10^{-4} & t_k \in (10, 80] \end{cases}.$$

Such kind of gradual-degradation may be caused by continuous wear or corrosion in the lifecycle,

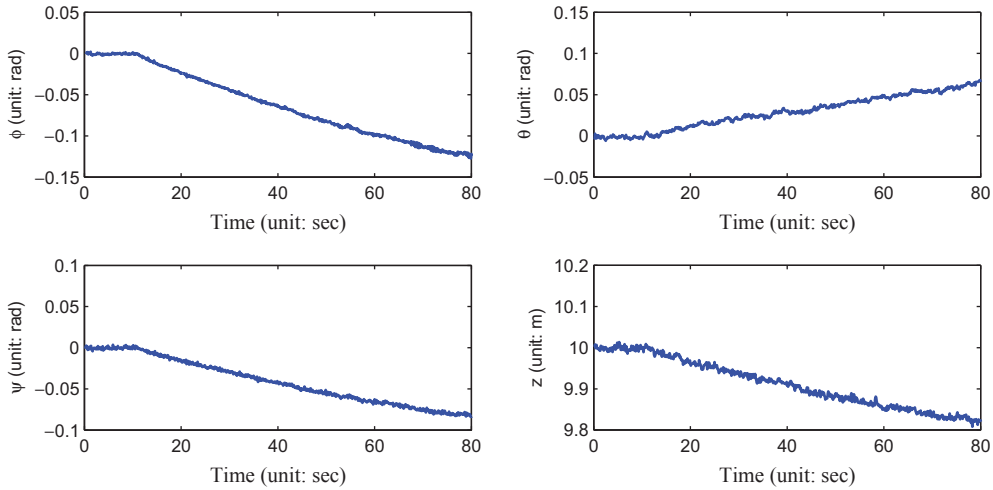


Fig. 6. Variations of ϕ, θ, ψ, z in gradual-degradation scenario. It is shown that the value of $[\phi, \theta, \psi, z]^T$ is relatively stable during the interval $[0, 10]$. After that, a gradual deviation of ϕ, θ, ψ, z is occurred due to gradual-degradation of actuator effectiveness.

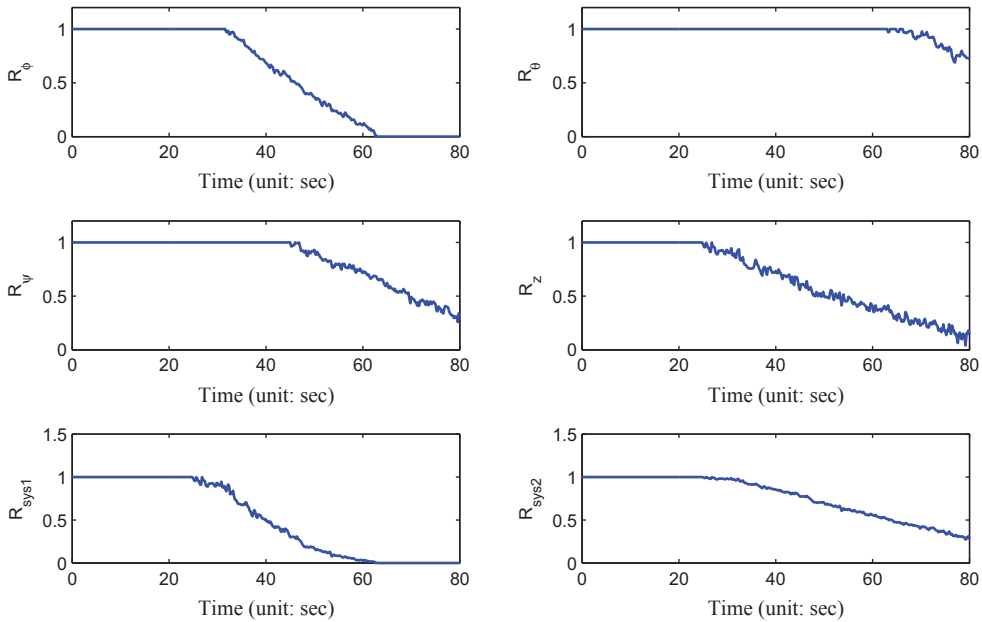


Fig. 7. PPR evaluation result in gradual-degradation scenario. The calculated PPRs of ϕ, θ, ψ, z decrease with different degree. Correspondingly, the PPR of the quadrotor gradually decreases, which indicates the performance degradation of quadrotor.

which is independent of fault occurrence. Actually, this part can be viewed as a simulation of accelerated aging experiment of quadrotors.

Under this scenario, Fig. 6 shows the variations of the SSVs ϕ, θ, ψ, z estimated by EKF. Furthermore, the calculated PPRs of ϕ, θ, ψ, z , and the quadrotor are depicted in Fig. 7.

In order to validate the proposed PPR-based performance prediction method, a 10-step SSVs' prediction is implemented by the Holt-Winters double exponen-

tial smoothing method. Then, the PPR is predicted in short-term based on the predicted distribution of SSVs. Figure 8 shows the 10-step prediction result of the SSVs ϕ, θ, ψ, z , and the corresponding PPR prediction result is depicted in Fig. 9. Note that a few data points that have not converged at the initial stage of prediction process are ignored here.

Remark 11. In reliability theory, the reliability curve of a product with no maintenance activities should

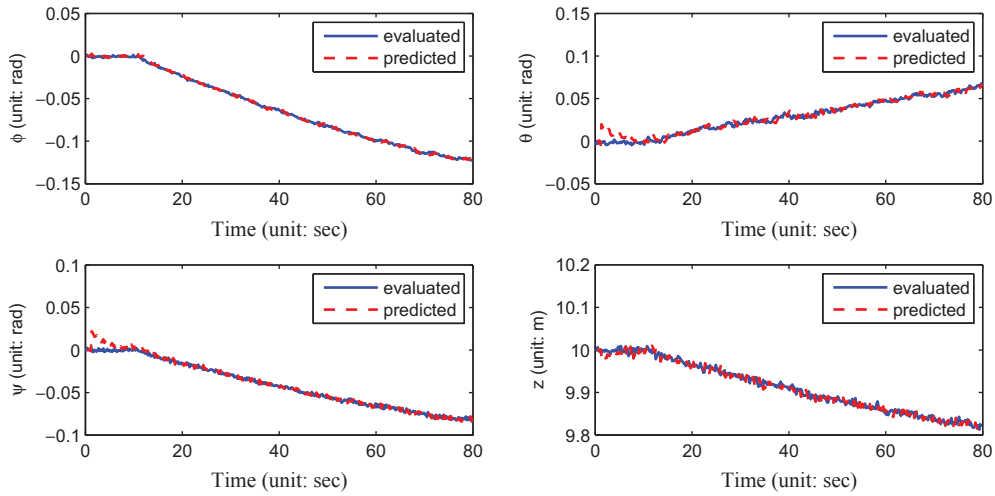


Fig. 8. 10-step prediction of ϕ , θ , ψ , z in gradual-degradation scenario. The blue solid line depicts the result of the PPR evaluation process, and the red dotted line depicts the result of the PPR prediction process.

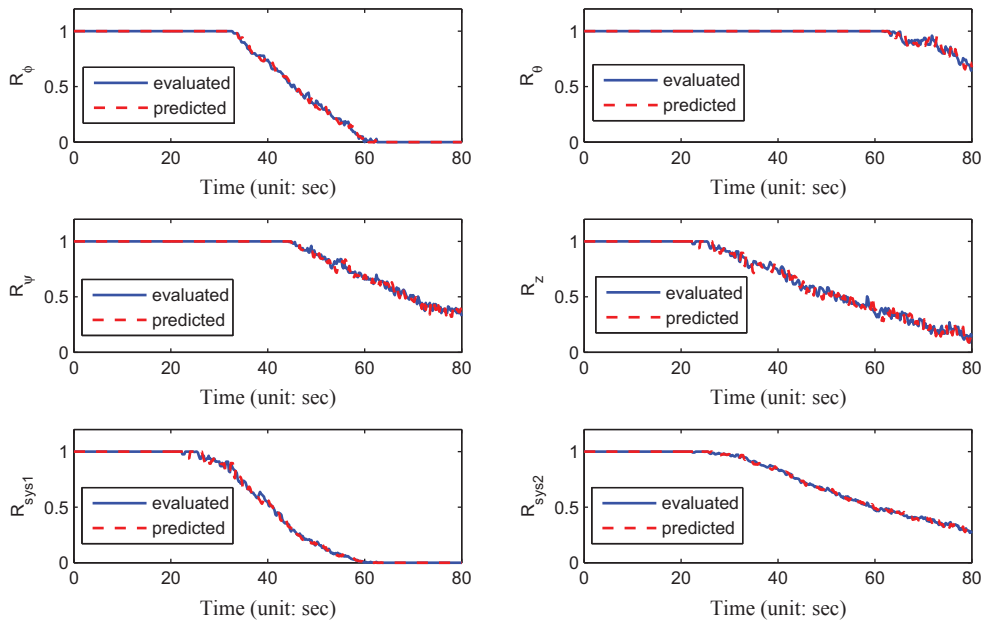


Fig. 9. 10-step PPR prediction in gradual-degradation scenario. The blue solid line depicts the result of the PPR evaluation process, and the red dotted line depicts the result of the PPR prediction process.

be monotonically non-increasing. However, in Figs. 5 and 7, the PPR curve has a non-increasing trend but with small fluctuations. That is because there exist system noise and measurement noise in the dynamic system, and these uncertainties will be brought into the variations of SSVs. The PPR presented in this paper aims to accurately reflect the real-time system performance based on real-time measuring data of the SSVs, which is different from the traditional reliability concept. Thus, it is rea-

sonable that the PPR curve fluctuates in a small range.

Remark 12. As shown in Fig. 7, the PPR calculation results of R_{sys1} and R_{sys2} are different. This is caused by the different definitions of quadrotor’s performance reliability presented in (23) and (24). Actually, both the results of R_{sys1} and R_{sys2} are able to characterize the performance of the quadrotor, acting as a reference for operation decision-making

and fault tolerant control under different mission requirements.

4.3. Summary

A simulation of quadrotor with partial loss of actuator effectiveness is presented to validate the availability and effectiveness of the proposed PPR-based performance evaluation and prediction method. In this simulation, a quadrotor's dynamic model is firstly presented. Then, the PPR-based system performance evaluation method is implemented under a fault-free scenario, a fixed-fault scenario, and a gradual-degradation scenario, respectively. Furthermore, the system performance is predicted in short-term under the gradual-degradation. The simulation results show that the system performance can be effectively evaluated by the proposed PPR-based algorithm. Meanwhile, the proposed PPR-based system performance prediction method is also easy to implement and effective with a high accuracy.

5. Conclusion

This paper proposes a modified PPR algorithm, which is then applied to the performance evaluation and prediction of dynamic systems. The simulation results show that the PPR is effectively evaluated to characterize the system performance, and the PPR prediction is also effectively achieved with tolerant errors. The advantages of the PPR based performance evaluation and prediction method presented in this paper are summarized in four aspects. First of all, the PPR has an ability to monitor real-time performance, and the modified PPR algorithm presented in this paper is convenient to implement in practice with higher real-time capability. Secondly, the SSV's real-time distribution obtained by EKF is used in PPR calculation rather than a single value, which reduces the uncertainties caused by system noise, observation noise and external disturbance. Thirdly, during the performance evaluation of dynamic systems by the proposed PPR algorithm, the system performance is determined on an integration of all SSVs' performance, which obtains a more comprehensive evaluation result. Finally, the modified PPR-based performance evaluation and prediction method is applied to a quadrotor in the simulation part. Actually, the proposed method can be also applied to other dynamic systems following the procedures presented in this paper. This indicates that the proposed PPR

algorithm has some degree of flexibility and robustness in performance evaluation and prediction. In future research, different prediction methods of SSVs distributions will be incorporated into the proposed PPR framework to satisfy system performance prediction under other fault patterns. Furthermore, the proposed method will be applied to the performance evaluation of other dynamic systems.

Acknowledgments

This work was supported by the National Natural Science Foundation of China under Grant 61473012.

References

- [1] G. Aaseng, A. Patterson-Hine and C. Garcia-Galan, A review of system health state determination methods, *Ist Space Exploration Conference*, 2005.
- [2] Y. Han and Y. Song, Condition monitoring techniques for electrical equipment—a literature survey, *IEEE Transactions on Power Delivery* **18**(1) (2003), 4–13.
- [3] H. Lu, W. Kolarik and S. Lu, Real-time performance reliability prediction, *IEEE Transactions on Reliability* **50**(4) (2011), 353–357.
- [4] S. Lu, H. Lu and W. Kolarik, Multivariate performance reliability prediction in real-time, *Reliability Engineering and System Safety* **72**(1) (2001), 39–45.
- [5] R. Chinnam, On-line reliability estimation for individual components using statistical degradation signal models, *Quality and Reliability Engineering International* **18**(1) (2002), 53–73.
- [6] Z. Xu, Y. Ji and D. Zhou, A new real-time reliability prediction method for dynamic systems based on on-line fault prediction, *IEEE Transactions on Reliability* **58**(3) (2009), 523–538.
- [7] Y. Kim and W. Kolarik, Real-time conditional reliability prediction from on-line tool performance data, *International Journal of Production Research* **30**(8) (1992), 1831–1844.
- [8] E. Myotyrri, U. Pulkkinen and K. Simola, Application of stochastic filtering for lifetime prediction, *Reliability Engineering and System Safety* **91**(2) (2006), 200–208.
- [9] J. Kharoufeh and S. Cox, Stochastic models for degradation based reliability, *IIE Transactions* **37**(6) (2005), 533–542.
- [10] X. Wang, P. Jiang, B. Guo and Z. Cheng, Real-time reliability evaluation with a general wiener process-based degradation model, *Quality and Reliability Engineering International* **30**(2) (2014), 205–220.
- [11] X. Wang, P. Jiang, B. Guo and Z. Cheng, Real-time reliability evaluation for an individual product based on change-point gamma and wiener process, *Quality and Reliability Engineering International* **30**(4) (2014), 513–525.
- [12] Z. Xu, Y. Ji and D. Zhou, Real-time reliability prediction for a dynamic system based on the hidden degradation process identification, *IEEE Transactions on Reliability* **57**(2) (2008), 230–242.
- [13] C. Hua, Q. Zhang, G. Xu, Y. Zhang and T. Xu, Performance reliability estimation method based on adaptive

- failure threshold, *Mechanical Systems and Signal Processing* **36**(2) (2013), 505–519.
- [14] K.-Y. Cai, *Introduction to Fuzzy Reliability*, Kluwer Academic Publishers, MA, USA, 1996.
- [15] K.-Y. Cai, C.Y. Wen and M.L. Zhang, Fuzzy variables as a basis for a theory of fuzzy reliability in the possibility context, *Fuzzy Sets and Systems* **42**(2) (1991), 145–172.
- [16] J. Purba, J. Lu, G. Zhang and W. Pedrycz, A fuzzy reliability assessment of basic events of fault trees through qualitative data processing, *Fuzzy Sets and Systems* **243** (2014), 50–69.
- [17] Z. Li and K.C. Kapur, Continuous-state reliability measures based on fuzzy sets, *IIE Transactions: Quality & Reliability Engineering* **44**(11) (2012), 1033–1044.
- [18] M. Bagheri, M. Miri and N. Shabakhty, Fuzzy reliability analysis using a new alpha level set optimization approach based on particle swarm optimization, *Journal of Intelligent & Fuzzy Systems* **30**(1) (2015), 235–244.
- [19] Y. Ding, M.J. Zuo and A. Lisnianski, Fuzzy multi-state systems general definition and performance assessment, *IEEE Transactions on Reliability* **57**(4) (2008), 589–594.
- [20] G. Mahapatra, B. Mahapatra and P. Roy, Fuzzy variable based fuzzy non-linear programming approach for optimization of complex system reliability, *Journal of Intelligent & Fuzzy Systems* **28**(4) (2015), 1899–1908.
- [21] M. Shafiq and R. Viertl, Empirical reliability functions based on fuzzy life time data, *Journal of Intelligent & Fuzzy Systems* **28**(2) (2015), 707–711.
- [22] Z. Zhao, Q. Quan, K.-Y. Cai and A. Profust, Reliability based approach to prognostics and health management, *IEEE Transactions on Reliability* **63**(1) (2014), 26–41.
- [23] G. Welch and G. Bishop, An Introduction to the Kalman Filter, UNC-CH Computer Science Technical Report 95041, 1995.
- [24] I. Miller, J. Freund and R. Johnson, Probability and statistics for engineers, Englewood Cliffs, NJ: Prentice-Hall, 1965.
- [25] H. Izadi, Y. Zhang and B. Gordon, Fault Tolerant, Model, Predictive Control of Quad-Rotor Helicopters with Actuator Fault Estimation, in *Proceedings of the 18th IFAC World Congress*, 2011, pp. 6343–6348.
- [26] I. Sadeghzadeh and Y. Zhang, A Review on Fault-Tolerant Control for Unmanned Aerial Vehicles (UAVs), in *Infotech Aerospace, AIAA 2011-1472*, 2011, pp. 1–12.
- [27] A. Chamseddine, D. Theilliol, Y. Zhang, C. Join and C. Rabbath, Active fault-tolerant control system design with trajectory re-planning against actuator faults and saturation: Application to a quadrotor unmanned aerial vehicle, *International Journal of Adaptive Control and Signal Processing* **29**(1) (2015), 1–23.
- [28] Z. Cen, H. Noura and Y. Younes, Robust, Fault Estimation on a Real Quadrotor UAV using Optimized Adaptive Thau Observer, in *International Conference on Unmanned Aircraft Systems*, 2013, pp. 550–556.
- [29] P. Lu, E. Kampen and B. Yu, Actuator Fault Detection, Diagnosis for Quadrotors, in *International Micro Air Vehicle Conference and Competition*, 2014, pp. 58–63.

- [30] M. Braun, *Differential Equations and Their Applications*, Springer Verlag, New York, 1978.

Appendix

A. Proof of Theorem 1

In order to prove *Theorem 1*, the key is to deduce the relationships among the transition probability $p_{ij}(t_0, t)$, the state probability $\varphi_{S_i}(t_0)$ at time t_0 , and the state probability $\varphi_{S_i}(t_k)$ at time t_k . Then, the item of transition probability can be replaced with the distribution of system's health status.

Suppose that the system performance is in a specific state $S_q \in U$ at time t_0 . Then, for $P(\bar{A} | B)$, firstly consider a special case that S_j can only move to S_{j-1} without passing via any intermediate state [14]. Then, it is obtained that

$$P(\bar{A} | B) = \sum_{j=1}^{q-1} \mu_{TSF}(m_{(j+1)j}) \cdot p_{(j+1)j}(t_0, t).$$

Since the system performance is in S_q at time t_0 , the system stays in S_j at time t implies that $m_{q(q-1)}, \dots, m_{(j+1)j}$ have already occurred during the time interval $[t_0, t]$. So,

$$p_{(j+1)j}(t_0, t) = \sum_{i=1}^j \varphi_{S_j}(t).$$

Further, note that if $\mu_F(S_i) < \mu_F(S_h) < \mu_F(S_j)$,

$$\mu_{TSF}(m_{ij}) = \mu_{TSF}(m_{ih}) + \mu_{TSF}(m_{hj}).$$

Then, Equation (25) at the bottom of the page can be obtained.

Equation (25) can be also applied to a general case [14]. According to *Assumption 1*, suppose that S_j can move to multiple worse states (not only to S_{j-1}) directly without passing via any intermediate state. Here, all the transition paths from S_q to S_1 can be enumerated. Suppose that there are M such paths. Note that the special case discussed above corresponds to $M = 1$. In this way,

$$P(\bar{A} | B) = \sum_{j=1}^{q-1} \left[\mu_{TSF}(m_{(j+1)j}) \cdot \left(\sum_{i=1}^j \varphi_{S_j}(t) \right) \right] \\ = \sum_{j=1}^{q-1} \left\{ \left[\mu_{TSF}(m_{qj}) - \mu_{TSF}(m_{q(j+1)}) \right] \cdot \left(\sum_{i=1}^j \varphi_{S_j}(t) \right) \right\} = \sum_{j=1}^{q-1} \mu_{TSF}(m_{qj}) \cdot \varphi_{S_j}(t). \quad (25)$$

$$\begin{aligned}
 & p_{ij}(t_0, t) \\
 &= \sum_{r=1}^M P \{ m_{ij} \text{ occurs during } [t_0, t] \text{ via path } r \} \\
 &= \sum_{r=1}^M p_{ij}^{(r)}(t_0, t).
 \end{aligned}$$

Suppose that there are N_r states in the r th path: $S_{N_r}^{(r)}, S_{N_r-1}^{(r)}, \dots, S_1^{(r)}$, where

$$l_{N_r}^{(r)} = q, l_1^{(r)} = 1.$$

Using the results when $M = 1$, Equation (26) at the bottom of the page can be obtained where

$$\varphi_{S_{j(r)}}(t) \begin{cases} \neq 0 & \text{if } S_j \text{ is contained in the } r\text{th path} \\ = 0 & \text{otherwise} \end{cases}.$$

So,

$$\begin{aligned}
 P(\bar{A} | B) &= \sum_{r=1}^M \sum_{j=1}^{q-1} \mu_{T_{SF}}(m_{qj}) \cdot \varphi_{S_{j(r)}}(t) \\
 &= \sum_{j=1}^{q-1} \sum_{r=1}^M \mu_{T_{SF}}(m_{qj}) \cdot \varphi_{S_{j(r)}}(t) \\
 &= \sum_{j=1}^{q-1} \mu_{T_{SF}}(m_{qj}) \cdot \varphi_{S_j}(t). \quad (27)
 \end{aligned}$$

Since the system performance is in a random state S_i at time t_0 with the probability of $\varphi_{S_i}(t_0)$, where

$$\begin{cases} \varphi_{S_i}(t_0) \geq 0 & S_i \in U \\ \sum_{i=1}^n \varphi_{S_i}(t_0) = 1 \end{cases}.$$

Nevertheless, when the system performance is in state S_1 at time t_0 , it is obtained that $P(\bar{A} | B) = 0$ due to $\mu_{T_{SF}}(m_{1j}) = 0$. Then, for other system states $S_i \in U$, it can be derived from (27) that

$$P(\bar{A} | B) = \sum_{i=2}^n \varphi_{S_i}(t_0) \cdot \left[\sum_{j=1}^{i-1} \mu_{T_{SF}}(m_{ij}) \cdot \varphi_{S_j}(t) \right]. \quad (28)$$

Then, substituting (28) into (1), it is obtained that

$$\begin{aligned}
 R(t) &= 1 - \left\{ \sum_{i=2}^n \varphi_{S_i}(t_0) \cdot \left[\sum_{j=1}^{i-1} \mu_{T_{SF}}(m_{ij}) \cdot \varphi_{S_j}(t) \right] \right\} \\
 &\quad \cdot \left[\sum_{i=1}^n \mu_S(S_i) \cdot \varphi_{S_i}(t_0) \right] - \sum_{i=1}^n \mu_F(S_i) \cdot \varphi_{S_i}(t_0).
 \end{aligned}$$

5.1. Proof of Corollary 1

Since the system performance is in state S_n at time t_0 , it is obtained that

$$P(B) = \sum_{i=1}^n \mu_S(S_i) \cdot \varphi_{S_i}(t_0) = \mu_S(S_n),$$

and

$$P(\bar{B}) = \sum_{i=1}^n \mu_F(S_i) \cdot \varphi_{S_i}(t_0) = \mu_F(S_n).$$

For $P(\bar{A} | B)$, consider the system performance is in state S_n at time t_0 ,

$$\varphi_{S_i}(t_0) = \begin{cases} 0 & i = 1, 2, \dots, n-1 \\ 1 & i = n \end{cases}. \quad (29)$$

Then, combining (28) and (29), it yields

$$P(\bar{A} | B) = \sum_{j=1}^{n-1} \mu_{T_{SF}}(m_{nj}) \cdot \varphi_{S_j}(t).$$

Then

$$\begin{aligned}
 R(t) &= 1 - P(\bar{A} | B) \cdot P(B) - P(\bar{B}) \\
 &= 1 - \left(\sum_{j=1}^{n-1} \mu_{T_{SF}}(m_{nj}) \cdot \varphi_{S_j}(t) \right) \\
 &\quad \cdot \mu_S(S_n) - \mu_F(S_n).
 \end{aligned}$$

$$\begin{aligned}
 P(\bar{A} | B) &= \sum_{r=1}^M \sum_{i=1}^q \sum_{j=1}^q \mu_{T_{SF}}(m_{ij}) \cdot p_{ij}^{(r)}(t_0, t) = \sum_{r=1}^M \sum_{j=1}^{N_r-1} \left[\mu_{T_{SF}}(m_{l_{j+1}^{(r)} l_j^{(r)}}) \cdot \left(\sum_{i=1}^j \varphi_{S_{l_i^{(r)}}}(t) \right) \right] \\
 &= \sum_{r=1}^M \sum_{j=1}^{N_r-1} \left\{ \left[\mu_{T_{SF}}(m_{l_{j+1}^{(r)} l_j^{(r)}}) - \mu_{T_{SF}}(m_{l_{N_r}^{(r)} l_{j+1}^{(r)}}) \right] \cdot \left(\sum_{i=1}^j \varphi_{S_{l_i^{(r)}}}(t) \right) \right\} \\
 &= \sum_{r=1}^M \sum_{j=1}^{N_r-1} \mu_{T_{SF}}(m_{l_{N_r}^{(r)} l_j^{(r)}}) \cdot \varphi_{S_{l_j^{(r)}}}(t) = \sum_{r=1}^M \sum_{j=1}^{q-1} \mu_{T_{SF}}(m_{qj}) \cdot \varphi_{S_{j(r)}}(t), \quad (26)
 \end{aligned}$$

Suppose $\mu_F(S_n) = 0$. Then

$$\begin{aligned} R(t) &= 1 - \sum_{j=1}^{n-1} \mu_{TSF}(m_{nj}) \cdot \varphi_{S_j}(t) \\ &= 1 - \sum_{j=1}^{n-1} (\mu_F(S_j) - \mu_F(S_n)) \cdot \varphi_{S_j}(t) \\ &= 1 - \sum_{j=1}^{n-1} \mu_F(S_j) \varphi_{S_j}(t) \\ &= 1 - \sum_{j=1}^n \mu_F(S_j) \varphi_{S_j}(t) \\ &= \sum_{j=1}^n \mu_S(S_j) \varphi_{S_j}(t). \end{aligned}$$

5.2. Proof of Corollary 2

Considering the system performance is in state S_q at time t_0 , it is obtained that

$$P(B) = \sum_{i=1}^n \mu_S(S_i) \cdot \varphi_{S_i}(t_0) = \mu_S(S_q),$$

and

$$P(\bar{B}) = \sum_{i=1}^n \mu_F(S_i) \cdot \varphi_{S_i}(t_0) = \mu_F(S_q).$$

Then, for (28), it is obtained that

$$\begin{aligned} P(\bar{A} | B) &= \sum_{j=1}^{q-1} \mu_{TSF}(m_{qj}) \cdot \varphi_{S_j}(t_k) \\ &= \mu_{TSF}(m_{qj}). \end{aligned}$$

Then

$$\begin{aligned} R(t) &= 1 - P(\bar{A} | B) \cdot P(B) - P(\bar{B}) \\ &= 1 - \mu_{TSF}(m_{qj}) \cdot \mu_S(S_q) - \mu_F(S_q) \\ &= \mu_S(S_q) \cdot (1 - \mu_{TSF}(m_{qj})). \end{aligned}$$

5.3. Membership functions used in the simulation

For the SSV $\phi \in [-\pi, \pi]$, we have the membership function of fuzzy success state as

$$\mu_S(\phi) = \begin{cases} \frac{\phi+0.1}{0.05} & \phi \in (-0.1, -0.05] \\ 1 & \phi \in (-0.05, 0.05] \\ \frac{\phi-0.1}{-0.05} & \phi \in (0.05, 0.1] \\ 0 & \phi \in (-\pi, -0.1] \cup (0.1, \pi) \end{cases},$$

and the membership function of fuzzy failure state is given as

$$\mu_F(\phi) = 1 - \mu_S(\phi).$$

In order to satisfy the condition $\mu_F(S_n) \leq \mu_F(S_{n-1}) \leq \dots \leq \mu_F(S_2) \leq \mu_F(S_1)$ in Section 2, the step of health status classification of ϕ is performed as

$$S_i = \left\{ \begin{array}{l} \phi \mid a_i \leq |\phi| < a_{i-1}; \\ \phi \in (-0.1, 0.1), i = 1, 2, \dots, n \end{array} \right\},$$

and

$$S_1 = \{\phi \mid 0.1 \leq |\phi| \leq \pi\},$$

where

$$\begin{aligned} \delta &= \frac{0.1}{n-1}, n = 100, a_i = 0.1 - (i-1)\delta, \\ & i = 1, \dots, n. \end{aligned}$$

For the SSVs θ and ψ , the fuzzy success/failure membership functions and the corresponding health status classification are identical to the form of ϕ . For the SSV z , the membership function of fuzzy success state is given as

$$\mu_S(z) = \begin{cases} \frac{z-9.8}{0.15} & z \in (9.8, 9.95] \\ 1 & z \in (9.95, 10.05] \\ \frac{z-10.2}{-0.15} & z \in (10.05, 10.2] \\ 0 & z \in [0, 9.8] \cup (10.2, +\infty) \end{cases},$$

and the membership function of fuzzy failure state is given as

$$\mu_F(z) = 1 - \mu_S(z).$$

The step of health status classification of z is performed as

$$S_i = \left\{ \begin{array}{l} z \mid a_i \leq |z - 10| < a_{i-1}; \\ z \in (9.8, 10.2), i = 2, 3, \dots, n \end{array} \right\},$$

and

$$S_1 = \{z \mid |z - 10| \geq 0.2, z \geq 0\},$$

where

$$\begin{aligned} \delta &= \frac{0.2}{n-1}, n = 100, \\ a_i &= 0.2 - (i-1)\delta, i = 1, \dots, n. \end{aligned}$$

Note that the membership function and the thresholds are determined on the basis of real flight data, and information of similar multicopters. Also, in practice, the thresholds are always adjusted according to the mission requirement and expert experience.